



A dual chemosensor for Zn²⁺ and Co²⁺ in aqueous media and living cells: Experimental and theoretical studies

Gyeong Jin Park^{a,b}, Jae Jun Lee^{a,b}, Ga Rim You^{a,b}, LeTuyen Nguyen^{c,d}, Insup Noh^{c,d}, Cheal Kim^{a,b,*}

^a Department of Fine Chemistry, Seoul National University of Science and Technology, Seoul 139-743, Republic of Korea

^b Department of Interdisciplinary Bio IT Materials, Seoul National University of Science and Technology, Seoul 139-743, Republic of Korea

^c Department of Chemical and Biomolecular Engineering, Seoul National University of Science and Technology, Seoul 139-743, Republic of Korea

^d Convergence Program of Biomedical Engineering and Biomaterials, Seoul National University of Science and Technology, Seoul 139-743, Republic of Korea

ARTICLE INFO

Article history:

Received 27 June 2015

Received in revised form

22 September 2015

Accepted 25 September 2015

Available online 28 September 2015

Keywords:

Fluorescence

Colorimetric

Determination of Zn ion

Determination of Co ion

Chemosensor

Cell imaging

ABSTRACT

A new versatile ‘dual’ chemosensor **1** has been synthesized for Zn²⁺ and Co²⁺. The sensor **1** comprises of quinoline as a fluorophore and N¹,N¹-dimethylethane-1,2-diamine as a water-soluble functional group. Sensor **1** showed a remarkable fluorescence enhancement in the presence of Zn²⁺ in aqueous solution. The sensor **1** also acted as a colorimetric sensor for Co²⁺ by changing its color from colorless to yellow. Importantly, the chemosensor **1** could be used to quantify Zn²⁺ and Co²⁺ in water samples and to image and quantify Zn²⁺ in living cells. Moreover, the sensing mechanisms of **1** for Zn²⁺ and Co²⁺ were supported by theoretical calculations. Therefore, this sensor has the ability to be a practical system for monitoring Zn²⁺ and Co²⁺ concentrations in biological systems and aqueous samples.

© 2015 Elsevier B.V. All rights reserved.

1. Introduction

Zinc is one of the most abundant transition-metal ions present in living cells, owing to its rich coordination chemistry [1–3]. Although most of the Zn²⁺ ions in a cell are tightly bound to metalloproteins, free forms are also found throughout the cell [4,5]. In the brain, 5–20% of the total Zn²⁺ is stored in presynaptic vesicles, and the highest intracellular free Zn²⁺ is found in the hippocampus [6,7]. Zn²⁺ modulates brain excitability and plays a key role in synaptic plasticity [8,9]. On the other hand, an excess amount of Zn²⁺ can have various detrimental effects on the nervous system. Many severe neurological diseases such as amyotrophic lateral sclerosis, Alzheimer’s disease, hypoxia ischemia, Parkinson’s disease, infantile diarrhea, and epilepsy are known to closely associate with dysregulation of zinc homeostasis [10–14]. In addition, an excess of zinc in the environment may reduce the soil microbial activity which results in phytotoxic effect [15–19]. Therefore, selective

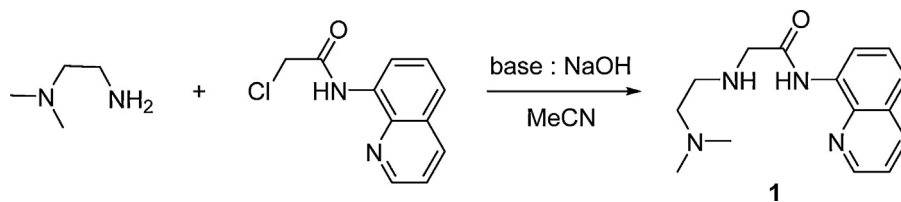
detection and quantification for zinc ion in environmental and biological systems have attracted growing attention of researcher.

Cobalt is an important micronutrient for animals and plants, and a major component of vitamin B₁₂ and other biological compounds [20–23]. A deficiency of cobalt may cause anemia, retarded growth and loss of appetite [24,25]. On the other hand, Co²⁺ pollution of environmental water causes severe effects on humans and animals. The toxicological effects of Co²⁺ on human beings include various diseases and disabilities such as asthma, decreased cardiac output, cardiac enlargement, heart disease, lung disease, dermatitis and vasodilation [26]. Therefore, the determination of trace amounts of Co²⁺ in environmental samples is also essential.

A variety of traditional methods (e.g. inductively coupled plasma atomic emission spectrometry, atomic absorption spectroscopy, and electrochemical methods) have been developed for analyses of zinc and cobalt in environmental samples and for diagnosis of their deficiencies in body tissue [27–32]. However, these methods require sophisticated instrumentations, tedious sample preparation procedures, and trained operators. By contrast, chemosensors are highly estimable means for the selective recognition of chemicals and biological species in environmental chemistry and biology [33]. The design and construction of chemosensors with high selectivity and sensitivity for trace metal ions, such as zinc and cobalt,

* Corresponding author at: Department of Interdisciplinary Bio IT Materials, Seoul National University of Science and Technology, Seoul 139-743, Republic of Korea.

E-mail address: chealkim@seoultech.ac.kr (C. Kim).



Scheme 1. Synthesis of sensor 1.

are currently of great importance as they allow nondestructive and prompt detection of metal ions by simple absorbance and fluorescence enhancement (turn-on) responses [33,34]. Among the various types of chemosensors, the chromogenic chemosensors are widely used owing to the inexpensive equipment required or no equipment at all [35]. Furthermore, fluorescence sensors are excellent tools for detecting metal ions due to their high sensitivity, good selectivity, high response speed and simple operation [36–44].

In view of this requirement we directed our efforts toward developing a chemosensor for zinc and cobalt ion recognitions. Specifically, the current work involved the synthesis, characterization and sensing properties of a new chemosensor **1** toward Zn^{2+} and Co^{2+} ions. To design **1**, we considered the combination of a quinoline moiety, a fluorophore with desirable photo-physical properties, and dimethylethane-1,2-diamine as a binding receptor (Scheme 1). In particular, we expected that the dimethylethane-1,2-diamine group, being hydrophilic in nature would increase water-solubility of the chemosensor. Therefore, the chemosensor **1** consisted of an organic π -conjugated compound with an electronic donor ($-NH$ group) group and an acceptor (quinoline) part with high electron affinity. Both groups were connected by single and double bonds, which featured a strong intramolecular charge transfer (ICT) character with broad and intense absorption bands in the visible spectral range.

Sensor **1** showed an intense fluorescence enhancement in the presence of zinc ions and a distinct color change in the presence of cobalt ions in near-perfect aqueous solution. Moreover, Zn^{2+} and Co^{2+} in water samples, and Zn^{2+} in living cells could be quantitatively determined by **1** for practical purposes.

2. Experimental

2.1. Materials and instrumentation

All the solvents and reagents (analytical grade and spectroscopic grade) were obtained commercially and used as received. NMR spectra were recorded on a Varian 400 MHz spectrometer. Chemical shifts (δ) were reported in ppm, relative to tetramethylsilane $Si(CH_3)_4$. Absorption spectra were recorded at 25 °C using a Perkin Elmer model Lambda 2S UV/Vis spectrometer. The emission spectra were recorded on a Perkin-Elmer LS45 fluorescence spectrometer. Electrospray ionization mass spectra (ESI-MS) were collected on a Thermo Finnigan (San Jose, CA, USA) LCQTM Advantage MAX quadrupole ion trap instrument. Elemental analysis for carbon, nitrogen, and hydrogen was carried out by using a Flash EA 1112 elemental analyzer (thermo) in Organic Chemistry Research Center of Sogang University, Korea.

2.2. Synthesis of sensor 1

2-Chloro-*N*-(quinolin-8-yl)acetamide (5 mmol, 1.11 g) and potassium iodide (8 mmol, 1.33 g) were dissolved in acetonitrile (MeCN, 8 mL) and stirred for 10 min. *N*¹,*N*¹-dimethylethane-1,2-diamine (5.5 mmol, 0.63 mL) and sodium hydroxide (6 mmol, 0.24 g) were added in the resulting solution. It was stirred for 6 h at room temperature. The solvent was removed under reduced

pressure to obtain brown oil, which was purified by silica gel column chromatography (9:1 v/v CH_2Cl_2 – CH_3OH) (Scheme 1). Yield: 0.98 g (72%). ¹H NMR (400 MHz, $DMSO-d_6$, 25 °C): δ = 11.39 (s, 1H), 8.92 (d, J = 4 Hz, 1H), 8.70 (d, J = 6 Hz, 1H), 8.40 (d, J = 8 Hz, 1H), 7.66 (d, J = 8 Hz, 1H), 7.62 (t, J = 4 Hz, 1H), 7.58 (t, J = 8 Hz, 1H), 3.41 (s, 2H), 2.70 (t, J = 8 Hz, 2H), 2.46 (t, J = 6.4 Hz, 2H), 2.17 (s, 6H) ppm. ¹³C NMR (100 MHz, $DMSO-d_6$, 25 °C): 170.71, 148.92, 138.92, 136.42, 134.13, 127.80, 126.94, 122.06, 121.55, 115.38, 58.91, 53.36, 47.16, 45.19, 45.10. LRMS (ESI): m/z calcd for $C_{15}H_{20}N_4O-H^+ + Zn^{2+}$: 335.2; found 335.09. Elemental analysis calcd (%) for $C_{15}H_{20}N_4O$: C, 66.15; H, 7.40; N, 20.57; found: C, 66.52; H, 7.27; N, 20.81.

2.3. Fluoregenic Zn(II) Sensing

2.3.1. UV-vis titration of 1 with Zn^{2+}

Sensor **1** (0.41 mg, 0.0015 mmol) was dissolved in MeCN (0.5 mL) and 10 μ L of the sensor **1** (3 mM) were diluted to 2.990 mL bis-tris buffer solution (10 mM, pH 7.0) to make the final concentration of 10 μ M. $Zn(NO_3)_2$ (0.01 mmol) was also dissolved in bis-tris buffer solution (0.5 mL) and 0.6–7.2 μ L of the Zn^{2+} solution (5 mM) were transferred to separate sensor solutions (10 μ M, 3 mL). After mixing them for a few seconds, UV-vis spectra were taken at room temperature.

2.3.2. Fluorescence titration of 1 with Zn^{2+}

Sensor **1** (0.41 mg, 0.0015 mmol) was dissolved in MeCN (0.5 mL) and 10 μ L of the sensor **1** (3 mM) were diluted to 2.990 mL bis-tris buffer solution (10 mM, pH 7.0) to make the final concentration of 10 μ M. $Zn(NO_3)_2$ (0.01 mmol) was also dissolved in bis-tris buffer solution (0.5 mL) and 0.6–7.2 μ L of the Zn^{2+} solution (5 mM) were added to the sensor **1** solution (10 μ M, 3 mL) prepared above. After mixing them for a few seconds, fluorescence spectra were obtained at room temperature.

2.3.3. Job plot measurement of Zn^{2+}

The sensor **1** (0.41 mg, 0.0015 mmol) and $Zn(NO_3)_2$ (0.0015 mmol) were separately dissolved in MeCN (0.5 mL). 300 μ L of the sensor **1** solution were diluted to 39.7 mL of buffer solution (10 mM bis-tris, pH 7.0) to make the concentration of 30 μ M. The $Zn(NO_3)_2$ solution was diluted in the same way. 5.0, 4.5, 4.0, 3.5, 3.0, 2.5, 2.0, 1.5, 1.0, 0.5 and 0 mL of the sensor **1** solution were taken and transferred to vials. 0, 0.5, 1.0, 1.5, 2.0, 2.5, 3.0, 3.5, 4.0, 4.5 and 5.0 mL of the Zn^{2+} solution were added to each sensor solution separately. Each vial had a total volume of 5 mL. After shaking the vials for a few seconds, UV-vis spectra were taken at room temperature.

2.3.4. NMR titration of 1 with Zn^{2+}

Four NMR tubes of **1** (0.55 mg, 0.002 mmol) dissolved in CD_3CN (0.5 mL) were prepared, and four different equivalents (0, 0.2, 0.5, and 1 equiv) of zinc nitrate dissolved in CD_3CN (0.5 mL) were added separately to the solutions of **1**. After shaking them for a few seconds, the ¹H NMR spectra were taken.

2.3.5. Determination of Zn²⁺ in water samples

Fluorescence spectral measurements of water samples containing Zn²⁺ were carried by adding 20 μ L of 3 mmol/L stock solution of **1** and 0.60 mL of 50 mmol/L bis-tris buffer stock solution to 2.38 mL sample solutions. After well mixed, the solutions were allowed to stand at 25 °C for 2 min before the test.

2.3.6. Methods of cell test of **1** with Zn²⁺

Human dermal fibroblast cells in low passage were cultured in FGM-2 medium (Lonza, Switzerland) supplemented with 10% fetal bovine serum, 1% penicillin/streptomycin in the in vitro incubator with 5% CO₂ at 37 °C. Cells were seeded onto a 8 well plate (SPL Life Sciences, Korea) at a density of 2×10^5 cells per well and then incubated at 37 °C for 4 h after addition of various concentrations (0–200 μ M) of Zn(NO₃)₂ dissolved in MeCN. After washing with phosphate buffered saline (PBS) two times to remove the remaining Zn(NO₃)₂, the cells were incubated with **1** (30 μ M) dissolved in MeCN for 30 min at room temperature. The cells were observed using a microscope (Olympus, Japan). The fluorescent images of the cells were obtained using a fluorescence microscope (Leica DMLB, Germany) at the excitation wavelength of 425 nm. The mean fluorescence intensity of the microscopy images was evaluated by Icy software [45].

2.3.7. Live/dead assay of fibroblast with **1**

To observe cell viability, a live and dead assay was performed for **1**. Fibroblasts ($P=5$) were in vitro cultured to reach 70% confluent. The cells were incubated with **1** (30 μ M) dissolved in MeCN for 1 h and 24 h, respectively. Reagent (400 μ L) of the live and dead assay was added into each cell culture plate. Both viability and morphological changes of the cells were observed by a fluorescence microscope (Leica DMLB, Leica; Wetzlar, Germany).

2.4. Chromogenic Co(II) sensing

2.4.1. UV–vis titration of **1** with Co²⁺

Sensor **1** (0.41 mg, 0.0015 mmol) was dissolved in MeCN (0.5 mL) and 30 μ L of the sensor **1** (3 mM) were diluted to 2.970 mL bis-tris buffer solution (10 mM, pH 7.0) to make the final concentration of 30 μ M. Co(NO₃)₂ (0.01 mmol) was also dissolved in bis-tris buffer solution (0.5 mL) and 1.8–21.6 μ L of the Co²⁺ solution (5 mM) were transferred to separate sensor solutions (30 μ M, 3 mL). After mixing them for a few seconds, UV–vis spectra were taken at room temperature.

2.4.2. Job plot measurement of Co²⁺

The sensor **1** (0.82 mg, 0.003 mmol) and Co(NO₃)₂ (0.003 mmol) were separately dissolved in MeCN (1 mL). 600 μ L of the sensor **1** solution were diluted to 39.4 mL of buffer solution (10 mM bis-tris, pH 7.0) to make the concentration of 60 μ M. The Co(NO₃)₂ solution was diluted in the same way. 5.0, 4.5, 4.0, 3.5, 3.0, 2.5, 2.0, 1.5, 1.0, 0.5 and 0 mL of the sensor **1** solution were taken and transferred to vials. 0, 0.5, 1.0, 1.5, 2.0, 2.5, 3.0, 3.5, 4.0, 4.5 and 5.0 mL of the Co²⁺ solution were added to each sensor solution separately. Each vial had a total volume of 5 mL. After shaking the vials for a few seconds, UV–vis spectra were taken at room temperature.

2.4.3. NMR titration of **1** with Co²⁺

Four NMR tubes of **1** (0.55 mg, 0.002 mmol) dissolved in CD₃CN (0.5 mL) were prepared, and four different equivalents (0, 0.2, 0.5, and 1 equiv) of cobalt nitrate dissolved in CD₃CN (0.5 mL) were added separately to the solutions of **1**. After shaking them for a few seconds, the ¹H NMR spectra were taken.

2.4.4. Determination of Co²⁺ in water samples

UV–vis spectral measurements of water samples containing Co²⁺ were carried by adding 30 μ L of 3 mmol/L stock solution of **1** and 0.60 mL of 50 mmol/L bis-tris buffer stock solution to 2.37 mL sample solutions. After well mixed, the solutions were allowed to stand at 25 °C for 2 min before the test.

2.4.5. Theoretical calculation methods

All DFT/TDDFT calculations based on the hybrid exchange–correlation functional B3LYP [46,47] were carried out using Gaussian 03 program [48]. The 6-31G** basis set [49,50] was used for the main group elements, whereas the LanL2DZ effective core potential (ECP) [51,52] was employed for Zn and Co. In vibrational frequency calculations, there was no imaginary frequency for the optimized geometries of **1**, **1**–Zn²⁺ and **1**–Co³⁺, suggesting that these geometries represent local minima. For all calculations, the solvent effect of water was considered by using the Cossi and Barone's CPCM (conductor-like polarizable continuum model) [53,54]. To investigate the electronic properties of singlet excited states, time-dependent DFT (TDDFT) was performed in the ground state geometries of **1**, **1**–Zn²⁺ and **1**–Co³⁺. Thirty lowest singlet states were calculated and analyzed. The GaussSum 2.1 [55] was used to calculate the contributions of molecular orbital in electronic transitions.

3. Results and discussion

3.1. Synthesis of **1**

We synthesized the new sensor **1** by following the general route of bonding a fluorophore to a metal chelating group (Scheme 1). The sensor **1** contained both the quinoline fluorophore and the dimethylethane-1,2-diamine metal chelating groups. Although this molecule is one of the quinoline fluorophore-based sensors, it has a dimethylethane-1,2-diamine group in place of various benzene ring moieties. The diamine functional group could be predicted to lead to a higher water-solubility than other quinolone fluorophore based sensors [56–58]. This sensor was characterized by ¹H NMR, ¹³C NMR, ESI-mass spectrometry and elemental analysis.

3.2. Fluorescence and absorption spectroscopic studies of **1** toward Zn²⁺

The fluorescence selectivity of **1** toward various metal ions was first studied in bis-tris buffer solution (10 mM, pH 7.0, Fig. 1). **1** alone has a weak fluorescence emission ($\lambda_{\text{max}} = 480$ nm and $\lambda_{\text{ex}} = 350$ nm). When 1 equiv of metal ions such as Na⁺, K⁺, Mg²⁺, Ca²⁺, Al³⁺, Cr³⁺, Mn²⁺, Fe²⁺, Fe³⁺, Co²⁺, Ni²⁺, Cu²⁺, Cd²⁺, Hg²⁺ and Pb²⁺ was added to the sensor **1**, it was found that the solution of **1** either exhibited no or a small significant increase in fluorescence. By contrast, the addition of Zn²⁺ into **1** showed a remarkable fluorescence enhancement (34 folds). Importantly, **1** can clearly distinguish Zn²⁺ from Cd²⁺, where such distinction of Zn²⁺ from Cd²⁺ is a well-known challenge. These results indicated that sensor **1** could be used as a fluorescence chemosensor for Zn²⁺.

To further investigate the chemosensing properties of **1**, fluorescence titration of **1** with Zn²⁺ ion was performed. As shown in Fig. S1, the emission intensity of **1** at 480 nm gradually increased until the amount of Zn²⁺ reached 1 equiv. The photophysical properties of **1** were also examined using UV–vis spectrometry. UV–vis absorption spectrum of **1** showed two absorption bands at 237 and 300 nm (Fig. S2). Upon the addition of Zn²⁺ ions to a solution of **1**, the two bands red-shifted to 250 and 345 nm, respectively. Meanwhile, two clear isosbestic points were observed at 267 and 320 nm, implying the undoubted conversion of free **1** to a zinc complex.

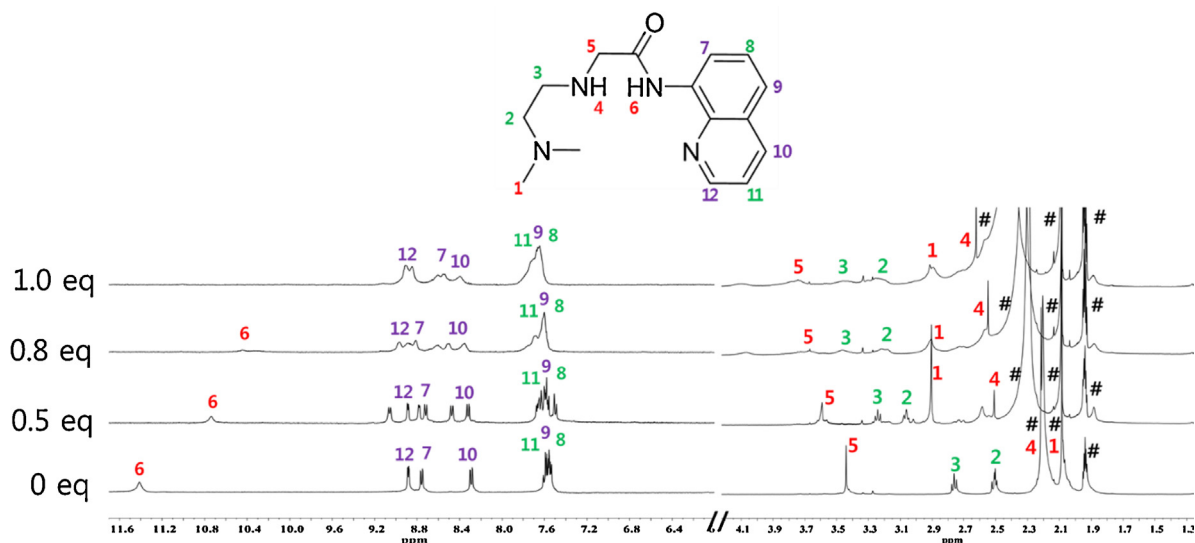


Fig. 4. ^1H NMR titration of **1** with $\text{Zn}(\text{NO}_3)_2$.

sensor which could distinguish Zn^{2+} from Cd^{2+} , both commonly having similar chemical properties.

3.3. ^1H NMR spectroscopic studies of **1** toward Zn^{2+}

The ^1H NMR titration experiments were studied to further examine the binding mode between **1** and Zn^{2+} ion (Fig. 4). Upon addition of 1.0 equiv of Zn^{2+} , the proton of the amide moiety (H_6) disappeared completely. The protons H_1 , H_2 , H_3 , H_4 , and H_5 showed downfield shifts, while up-field shifts were observed for H_7 and H_{12} . Other protons in **1** changed a little. These chemical shifts suggested that the deprotonated nitrogen atom of the amide moiety and the three nitrogen atoms might coordinate to Zn ion (Scheme 2). This coordinative behavior of the five-membered ring formed by Zn^{2+} and sensor **1** was previously observed in similar type of zinc complexes [57]. There was no shift in the position of proton signals on further addition of Zn^{2+} (>1.0 equiv), which indicated a 1:1 ratio of **1**– Zn^{2+} complex. Therefore, based on fluorescence titration, UV–vis titration, Job plot, ESI-mass spectrometry analysis, ^1H NMR titration, and the crystal structures of similar types of zinc complexes reported earlier, a 1:1 binding structure of **1**– Zn^{2+} complex can be proposed, as shown in Scheme 2.

3.4. pH Effect of **1** toward Zn^{2+}

To study the practical applicability of this chemosensor, the effects of pH on the fluorescence response of Zn^{2+} were investigated (Fig. S5). The fluorescence spectra of sensor **1** in the absence and presence of 1 equiv of Zn^{2+} were examined at various pH ranging from 3 to 12. The fluorescence intensity of **1** in the presence of Zn^{2+} showed a significant response between pH 6 and 12. These results indicated that Zn^{2+} could be clearly detected by the fluorescence spectral measurement using **1** over environmentally and physiologically relevant pH range (pH 6.0–8.4) [69–71], especially for monitoring Zn^{2+} in water samples and living cells.

3.5. Reversible test of **1** toward Zn^{2+} by using EDTA

To examine the reversibility of sensor **1** toward Zn^{2+} in buffer solution, ethylenediaminetetraacetic acid (EDTA, 1 equiv) was added to the complexed solution of sensor **1** and Zn^{2+} . As shown in Fig. 5, the fluorescence of the **1**– Zn^{2+} complex was immediately quenched. Upon addition of Zn^{2+} again, the fluorescence

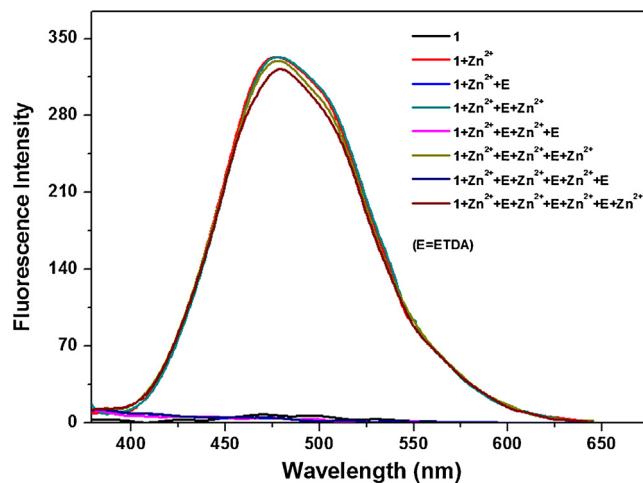


Fig. 5. Fluorescence spectral changes of **1** ($10\ \mu\text{M}$) after the sequential addition of Zn^{2+} and EDTA in buffer solution ($10\ \text{mM}$ bis-tris, pH 7.0).

was recovered. The fluorescence emission changes were almost reversible even after several cycles with the sequential alternative addition of Zn^{2+} and EDTA. These results indicated that sensor **1** could be recycled simply through treatment with a proper reagent such as EDTA. Such reversibility and regeneration are practically important in the fabrication of chemosensors to sense Zn^{2+} .

3.6. Analytical figures of merit

We constructed a calibration curve for the determination of Zn^{2+} by **1** (Fig. S6). A good linear relationship was observed between the fluorescence intensity of **1** and Zn^{2+} concentration (0.00 – $15.00\ \mu\text{M}$) with a correlation coefficient of $R^2 = 0.9921$ ($n = 3$), which means that **1** is suitable for quantitative detection of Zn^{2+} . The detection limit has also been calculated as $0.01\ \mu\text{M}$ based on the definition by IUPAC ($\text{C}_{\text{DL}} = 3S_b/m$), which is much lower than the WHO guideline ($76\ \mu\text{M}$) for Zn^{2+} ions in drinking water [33]. The value of the detection limit was compatible with those of previously reported zinc chemosensors in aqueous solution, as shown in Table S1.

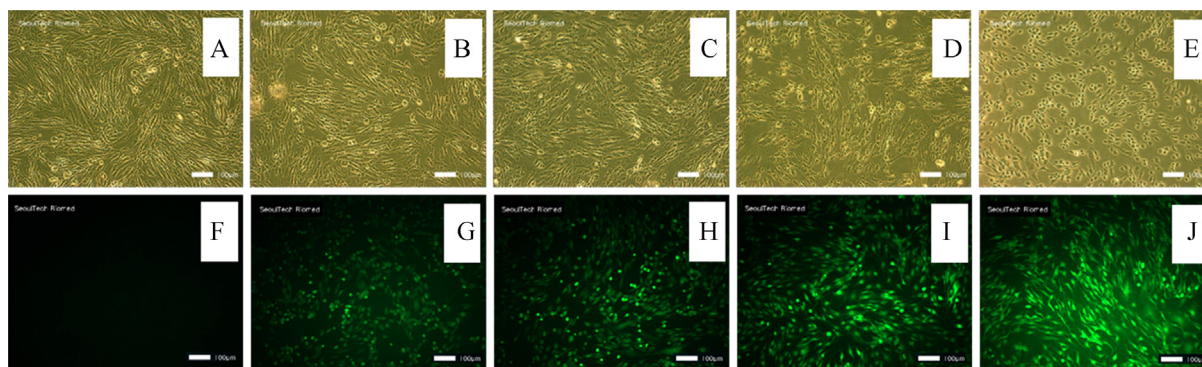


Fig. 6. Fluorescence images of fibroblasts cultured with Zn^{2+} and **1**. Cells were exposed to 0 (A and F), 40 (B and G), 60 (C and H), 100 (D and I) and 200 μM (E and J) $\text{Zn}(\text{NO}_3)_2$ for 4 h and then later with **1** (30 μM) for 30 m. The top images (A–E) were observed under light microscope and the bottom images (F–J) were recorded through a fluorescence microscope. The scale bar is 100 μm .

Table 1
Determination of Zn(II) in water samples.

Sample	Zn(II) added ($\mu\text{mol/L}$)	Zn(II) found ($\mu\text{mol/L}$)	Recovery (%)	R.S.D. (n = 3) (%)
Tap water	0.00	0.00		
	6.00	6.61	110.2	1.7
Water sample ^a	0.00	3.97	99.3	4.9

^a Synthesized by deionized water, 4.00 $\mu\text{mol/L}$ Zn(II), 10 $\mu\text{mol/L}$ Cd(II), Pb(II), Na(I), K(I), Ca(II), Mg(II). Conditions: [**1**] = 20 $\mu\text{mol/L}$ in 10 mM bis-tris buffer-MeCN solution (999:1, pH 7.0).

3.7. Determination of zinc ion in water samples

In order to examine the practical applicability of **1** for environmental samples, the chemosensor was further used for the determination of Zn^{2+} in tap water samples. As shown in Table 1, a satisfactory recovery and R.S.D. values of water samples were obtained. Moreover, we prepared artificially polluted water samples by adding various metal ions known as being involved in industrial processes into deionized water. The results were also summarized in Table 1, which showed a satisfactory recovery and R.S.D. values for all the water samples.

3.8. Biological application of **1** in detecting Zn^{2+}

To further demonstrate the potential of **1** to monitor Zn^{2+} in living matrices, fluorescence imaging experiments were carried out in living cells (Fig. 6). Adult human dermal fibroblasts were first incubated with various concentrations of aqueous Zn^{2+} solutions (0, 40, 60, 100 and 200 μM) for 4 h and then exposed to **1** for 30 min before imaging. The fibroblasts that were cultured with both Zn^{2+} and **1** exhibited fluorescence (Fig. 6), while those cells cultured without Zn^{2+} or without **1** did not exhibit any

fluorescence. The intensity and region of the fluorescence within the cell with **1** increased as the Zn^{2+} concentration increased from 20 to 200 μM . The mean fluorescence intensity of the microscopy image in Fig. 6 was evaluated by Icy software (Fig. S7). The detection limit obtained was 0.01 μM , which was identical to that obtained for Zn^{2+} in the drinking water (Fig. S7). In order to further confirm that the increase in the fluorescence depends on the concentrations of Zn^{2+} , the Zn^{2+} -supplemented cells (Fig. 7B) were treated with 400 μM of EDTA to remove the intracellular levels of Zn^{2+} . The intracellular fluorescence nearly disappeared with the EDTA chelation (Fig. 7C), demonstrating that the observed intracellular fluorescence enhancement (Fig. 7B) was due to the changing levels in the Zn^{2+} -supplemented cells. Moreover, the biocompatibility of **1** was also examined with the living cells (Fig. S8). All the fibroblasts were still alive for 24 h. These observations confirmed that **1** can be a suitable and biocompatible sensor to detect Zn^{2+} in living cells.

3.9. Absorption spectroscopic studies of **1** toward Co^{2+}

The colorimetric sensing ability of **1** was also examined with various metal ions such as Na^+ , K^+ , Mg^{2+} , Ca^{2+} , Cr^{3+} , Mn^{2+} , Fe^{2+} , Fe^{3+} , Co^{2+} , Ni^{2+} , Cu^{2+} , Zn^{2+} , Cd^{2+} , Al^{3+} , and Pb^{2+} in buffer solution (10 mM bis-tris, pH 7.0) at room temperature. The presence of Fe^{2+} , Fe^{3+} , Zn^{2+} , Cu^{2+} and Co^{2+} led to a redshift of the absorption maxima of **1** to different extents, while the sensor **1** showed almost no change in absorption peak in the presence of other metal ions (Fig. 8a). Most importantly, only Co^{2+} showed not only a distinct spectral change (Fig. 8a) but also a color change from colorless to yellow (Fig. 8b), indicating that **1** can serve as a chemosensor for a “naked-eye” detection of Co^{2+} in fully aqueous solution. To the best of our knowledge, the current work shows for the first time that chemosensor **1** can detect both Zn^{2+} and Co^{2+} by different sensing methods in fully aqueous solution [11–26].

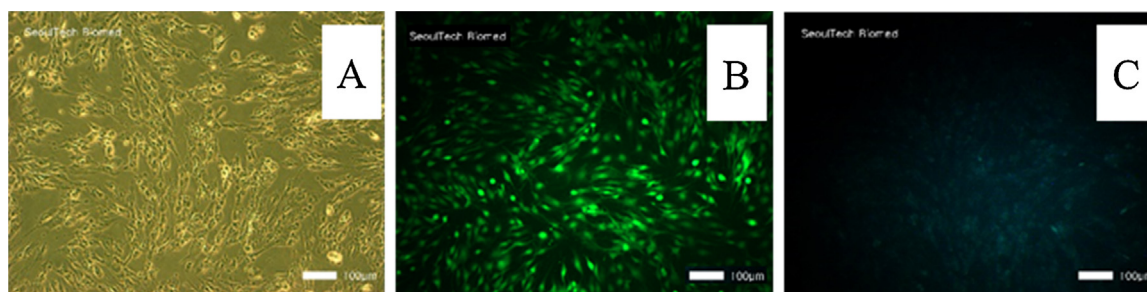


Fig. 7. Fluorescence images of fibroblasts sequentially cultured with Zn^{2+} , **1**, and EDTA. (A) A light image of fibroblasts with **1**. (B) Cell was exposed to 100 μM Zn^{2+} for 4 h and then with 30 μM **1** for 1 h. Fluorescence image of (C) cell was taken 40 min after (B) cell was exposed to 400 μM of EDTA. (B) and (C) were recorded using a fluorescence microscope, and (A) was observed under a light microscope. The scale bar is 100 μm .

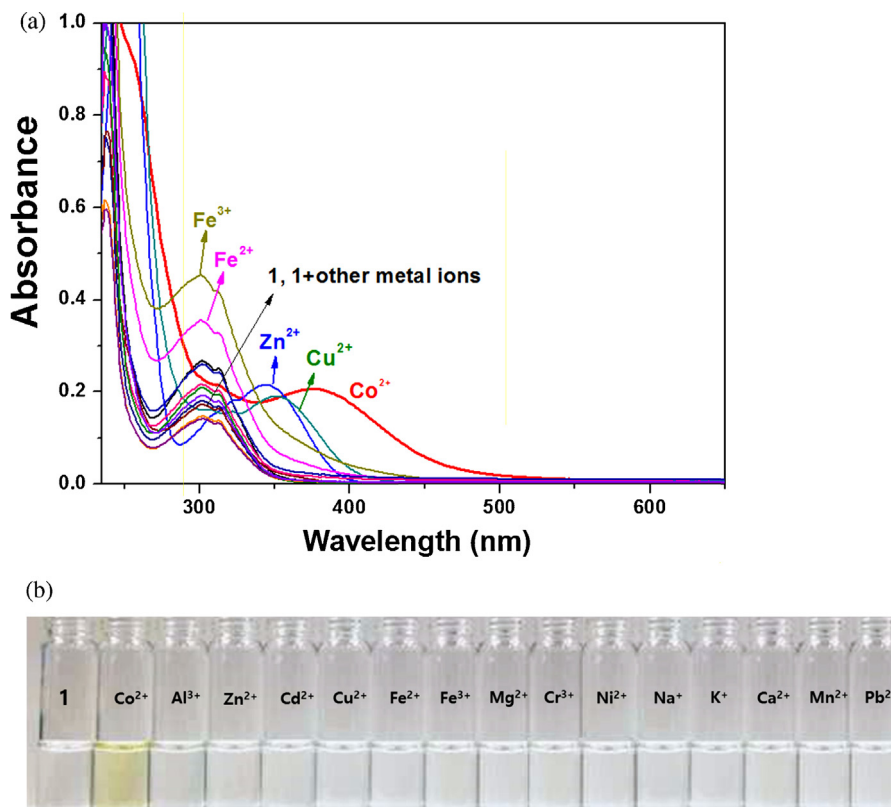


Fig. 8. (a) UV–vis spectral changes of **1** ($60\ \mu\text{M}$) upon addition of 1 equiv of various metal ions such as Na^+ , K^+ , Mg^{2+} , Ca^{2+} , Al^{3+} , Cr^{3+} , Mn^{2+} , Fe^{2+} , Fe^{3+} , Co^{2+} , Ni^{2+} , Cu^{2+} , Zn^{2+} , Cd^{2+} , and Pb^{2+} in buffer solution (10 mM bis-tris, pH 7.0). (b) Colorimetric changes of **1** ($60\ \mu\text{M}$) upon the addition of various metal ions (1 equiv) in buffer solution (10 mM bis-tris, pH 7.0).

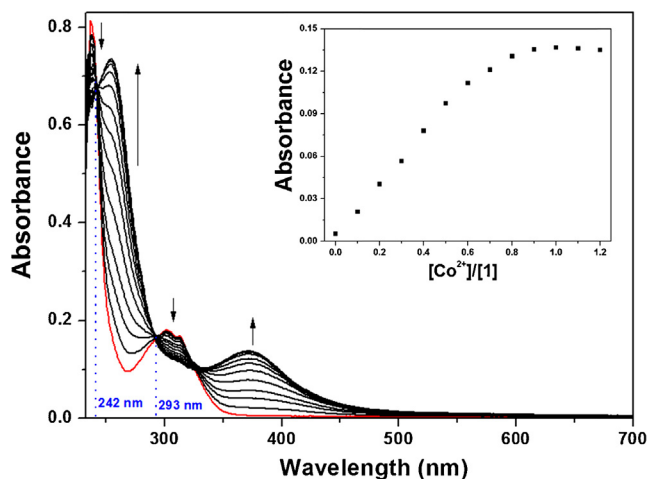


Fig. 9. UV–vis absorption spectra of **1** ($30\ \mu\text{M}$) obtained during the titration by the range of 0–1.2 equiv of $\text{Co}(\text{NO}_3)_2$ in bis-tris buffer solution at room temperature. Inset: absorption intensity at 370 nm versus the number of equiv of Co^{2+} added.

To further investigate the chemosensing properties of **1**, UV–vis titration of **1** with Co^{2+} was performed (Fig. 9). Upon the addition of Co^{2+} to a solution of **1**, the two absorbance peaks at 237 and 300 nm gradually decreased and two new absorption peaks at 267 and 370 nm appeared concomitantly. This red shift may originate from the Co^{2+} coordination-enhanced LMCT effect [72], which resulted in the red shifts from 237 to 267 nm and from 300 to 370 nm. The new band at 267 nm was also observed to grow in intensity with

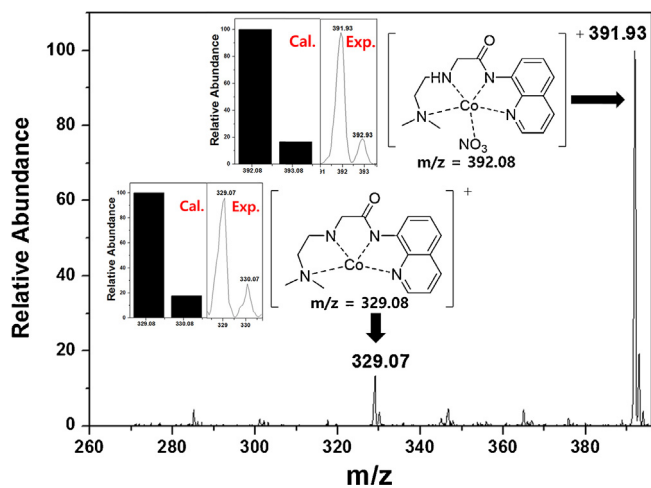
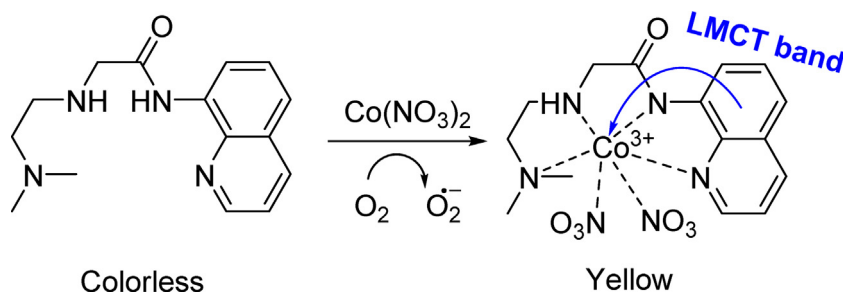


Fig. 10. Positive-ion electrospray ionization mass spectrum of **1** ($100\ \mu\text{M}$) upon addition of 1 equiv of Co^{2+} .

some metal ions including Zn^{2+} , while the band at 370 nm was only seen for cobalt. The distinct absorption at 370 nm might be the reason for the distinct yellow color of the sensor **1** solution containing Co^{2+} .

Job plot [65] analysis exhibited a 1:1 complexation stoichiometry for **1**– Co^{2+} complex (Fig. S9), which was further confirmed by ESI-mass spectrometric analysis (Fig. 10). Even though Co^{2+} was used as the standard metal ion, the ESI-mass spectrum showed the presence of only Co^{3+} complexes with 1:1 stoichiometry. A



Scheme 3. Proposed sensing mechanism of Co^{2+} by **1** and proposed structure of **1**- Co^{3+} complex.

peak at m/z 391.93 was assigned to $[\mathbf{1}-\text{H}^+ + \text{Co}^{3+} + \text{NO}_3^-]^+$ (calcd. 392.08) and the peak at m/z 329.07 assignable to $[\mathbf{1}-2\text{H}^+ + \text{Co}^{3+}]^+$ [calcd, 329.08] complex. To more clearly confirm our proposal of the oxidation of Co^{2+} to Co^{3+} in the **1**- Co^{2+} complex, we carried out the sensing test of **1**- Co^{2+} complexes under the degassed conditions. If there is no color change for the complexation of the Co^{2+} ion with **1** under the degassed conditions, it would mean that **1** detected Co^{3+} , not Co^{2+} , because **1**- Co^{2+} complex could be only oxidized to **1**- Co^{3+} complex by O_2 molecules in absence of other oxidants. Finally, we observed no color change for **1**- Co^{2+} complex under the degassed conditions. This result indicated that Co^{2+} was oxidized to Co^{3+} when binding to sensor **1** under aerobic conditions. Based on fluorescence titration, UV-vis titration, Job plot, ESI-mass spectrometry analysis, and the degassed experiments, we propose the 1:1 binding mode between **1** and Co^{2+} as shown in Scheme 3.

The association constant between **1** and Co^{2+} was determined as $4.0 \times 10^4 \text{ M}^{-1}$ through Li's equation (Fig. S10) [66], which is in the range of those (10^4 – 10^7) previously reported for Co^{2+} -binding chemosensors [21,26,73,74]. To examine the interference of other relevant metal ions on **1**- Co^{2+} complexation, the competition experiments were performed in the presence of Co^{2+} mixed with other metal ions such as Na^+ , K^+ , Mg^{2+} , Ca^{2+} , Cr^{3+} , Mn^{2+} , Fe^{2+} , Fe^{3+} , Ni^{2+} , Cu^{2+} , Zn^{2+} , Cd^{2+} , Al^{3+} , and Pb^{2+} (Fig. S11). There was either no or slight interference in the detection of Co^{2+} from various metal ions, while Zn^{2+} and Cu^{2+} did interfere with 72 and 88%.

3.10. ^1H NMR spectroscopic studies of **1** toward Co^{2+}

The ^1H NMR titration of Co^{2+} with **1** was conducted in air (Fig. S12). We expected that the **1**- Co^{2+} complex has a paramagnetic character, while the **1**- Co^{3+} complex with a strong-field N4-type ligand shows a diamagnetic character [75,76]. Upon the addition of Co^{2+} (1.0 equiv) into the **1** solution, the ^1H NMR spectrum of the cobalt complex indicated sharp signals, suggesting that a diamagnetic **1**- Co^{3+} complex formed. Further addition of Co^{2+} (>1 equiv) rendered the signals disappear due to a paramagnetic character of an excess Co^{2+} . These results led us to conclude that the **1**- Co^{2+} complex was oxidized to the low-spin **1**- Co^{3+} complex by oxygen. On the other hand, the proton of the amide moiety (H_6) disappeared completely upon addition of 1 equiv of Co^{2+} . The protons H_1 , H_2 , H_3 , and H_5 showed downfield shifts and other protons in **1** changed a little. These chemical shifts indicated that the deprotonated nitrogen atom of the amide moiety and the three nitrogen atoms might coordinate to Co ion (Scheme 3). Based on UV-vis titration, Job plot, ESI-mass spectrometry analysis, ^1H NMR titration, and the crystal structures of similar types of Co^{3+} complexes reported earlier, a 1:1 binding structure of **1**- Co^{3+} complex can be proposed, as shown in Scheme 3.

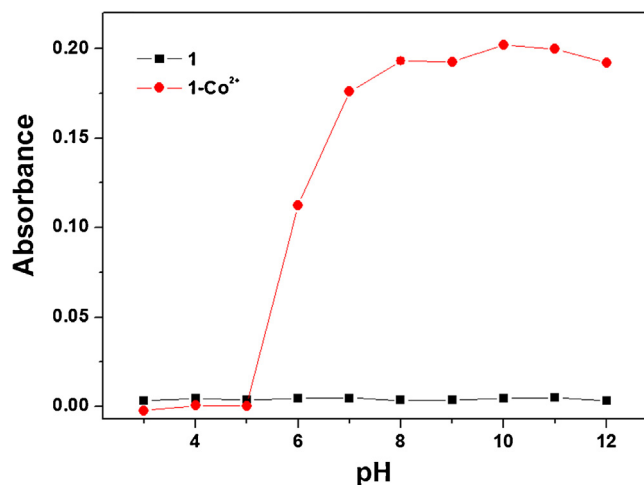


Fig. 11. Absorbance (at 370 nm) of **1** (60 μM) in the presence of Co^{2+} (1 equiv) at different pH values (3–12) in buffer solution (10 mM bis-tris, pH 7.0).

3.11. pH effect on the complexation of **1** and Co^{2+}

The effect of pH on the absorption response of receptor **1** to Co^{2+} ions was investigated in the pH range of 3–12 (Fig. 11). The color of the **1**- Co^{2+} complex exhibited the intense and stable absorption intensities between pH 6 and pH 12, which warrant that Co^{2+} could be clearly detected by simple naked eye or UV-vis absorption measurements using receptor **1** over a wide pH range of 6–12.

3.12. Analytical figures of merit

We plotted a calibration curve for the determination of Co^{2+} by **1** (Fig. S13). A good linear relationship was observed between the absorption intensity of **1** and Co^{2+} concentration (0.00–14.00 μM) with a correlation coefficient of $R^2 = 0.9968$ ($n = 3$), which means that **1** is suitable for quantitative detection of Co^{2+} . The detection limit was calculated as 6.89 μM based on the definition by IUPAC ($C_{\text{DL}} = 3S_b/m$), which is somewhat higher than that ($1.7 \times 10^{-5} \text{ M}$) recommended by environmental protection agency (EPA). In order to evaluate the practical applicability of **1** for environmental samples, the chemosensor was applied for the determination of Co^{2+} in both tap and drinking water samples. As shown in Table 2, a suitable recovery and R.S.D. values from the water samples were obtained.

3.13. Theoretical calculations for **1** with Zn^{2+} and Co^{2+}

To obtain a deeper insight into the sensing mechanism of Zn^{2+} and Co^{2+} with **1**, theoretical calculations were performed in parallel to the experimental studies. As Job plot, ESI-mass spectrometry analysis and ^1H NMR titration showed that **1** reacted with Zn^{2+} and Co^{2+} in a 1:1 stoichiometric ratio, respectively, all theoretical

Table 2
Determination of Co(II) in water samples.

Sample	Co(II) added ($\mu\text{mol/L}$)	Co(II) found ($\mu\text{mol/L}$)	Recovery (%)	R.S.D. ($n = 3$) (%)
Tap water	0.00	0.00	99.8	2.58
	9.00	8.98		
Drinking water	0.00	0.00	100.3	2.51
	10.00	10.03		

Conditions: [1] = 20 $\mu\text{mol/L}$ in 10 mM bis-tris buffer-MeCN solution (999:1, pH 7.0).

calculations were performed with a 1:1 stoichiometry. As 1-Co²⁺ complex was oxidized to 1-Co³⁺ complex with a diamagnetic property, 1-Co³⁺ was optimized with the diamagnetic character ($S = 0$, DFT/B3LYP/main group atom: 6-31G** and Co: Lanl2DZ/ECP). The significant structural properties of the energy-minimized structures are shown in Fig. S14. The energy minimized structures of 1 indicated the intramolecular hydrogen bond of 1H and 2N or 3H and 4N. 1-Zn²⁺ complex showed that four nitrogen atoms of 1 and one nitrate were coordinated to Zn²⁺. 1-Co³⁺ complex showed that four nitrogen atoms of 1 and two nitrates were coordinated to Co³⁺.

To further understand the sensing mechanisms of 1 toward Zn²⁺ and Co²⁺, we compared the frontier molecular orbitals of 1, 1-Zn²⁺ and 1-Co³⁺ (Fig. S15). In case of 1, the energy gap between HOMO to LUMO was assigned to ICT band (286.73 nm) from the dimethylamine moiety to the quinoline one. The energy gap between HOMO to LUMO for 1-Zn²⁺ complex was assigned to $\pi \rightarrow \pi^*$ transition (330.10 nm) of the quinoline, which acted as fluorophore. These results indicated the red shift of UV-vis spectrum and the enhancement of fluorescence when 1 was coordinated to Zn²⁺. The energy gap between HOMO to LUMO for 1-Co³⁺ was assigned to ligand-to-metal charge-transfer (LMCT) from quinoline to Co [72], which indicated the red shifted energy (386.20 nm) compared to 1. In addition, LMCT provides a pathway for non-radiative decay of the excited state, which induces the turn-off fluorescent change of 1. Thus, there was no fluorescence enhancement of 1-Co³⁺ complex.

4. Conclusion

A new dual sensor based on dimethylethane-1,2-diamine and quinolone had been synthesized. The sensor 1 exhibited a high sensitivity and excellent selectivity toward Zn²⁺ over competing relevant metal ions in a fully aqueous solution. The binding of the sensor 1 and Zn²⁺ was chemically reversible with EDTA. Importantly, the recovery studies of the water samples added with Zn²⁺ and the living cell experiments demonstrated its potential for practical applications. Moreover, 1 could act as a colorimetric sensor capable of distinguishing Co²⁺ from other metal ions in buffer solution. The chemosensor 1 could also be used to detect and quantify Co²⁺ in water samples with UV-vis spectroscopy. Furthermore, the sensing mechanisms for Zn²⁺ and Co²⁺ were explained by theoretical calculations. It is noteworthy that such a single chemosensor for the detection of both Zn²⁺ and Co²⁺ in a fully aqueous solution has been not reported to date, to the best of our knowledge. This study, thus provide a chemosensor that can be an example of 'a bimodal chemosensor for dual analytes' in near-perfect aqueous solution.

Acknowledgements

Financial support from Basic Science Research Program through the National Research Foundation of Korea (NRF) funded by the Ministry of Education, Science and Technology (NRF-2014R1A2A1A11051794 and NRF-2015R1A2A2A09001301) are gratefully acknowledged. We thank Nano-Inorganic Laboratory, Department of Nano & Bio Chemistry, Kookmin University to access the Gaussian 03 program packages.

Appendix A. Supplementary data

Supplementary data associated with this article can be found, in the online version, at <http://dx.doi.org/10.1016/j.snb.2015.09.129>.

References

- [1] A. Ajayaghosh, P. Carol, S. Sreejith, A ratiometric fluorescence probe for selective visual sensing of Zn²⁺, *J. Am. Chem. Soc.* 133 (2005) 14962–14963.
- [2] Y. Wu, X. Peng, B. Guo, J. Fan, Z. Zhang, J. Wang, A. Cui, Y. Gao, Boron dipyrromethene fluorophore based fluorescence sensor for the selective imaging of Zn(II) in living cells, *Org. Biomol. Chem.* 3 (2005) 1387–1392.
- [3] P. Jiang, L. Chen, J. Lin, Q. Liu, J. Ding, X. Gao, Z. Guo, Novel zinc fluorescent probe bearing dansyl and aminoquinoline groups, *Chem. Commun.* (2002) 1424–1425.
- [4] A. Loas, R.J. Radford, S.J. Lippard, Addition of a second binding site increases the dynamic range but alters the cellular localization of a red fluorescent probe for mobile zinc, *Inorg. Chem.* 53 (2014) 6491–6493.
- [5] K. Tayade, B. Bondhopadhyay, H. Sharma, A. Basu, V. Gite, S. Attarde, N. Singh, A. Kuwar, "Turn-on" fluorescent chemosensor for zinc(II) dipodal ratiometric receptor: application in live cell imaging, *Photochem. Photobiol. Sci.* 13 (2014) 1052–1057.
- [6] J.H. Weiss, S.L. Sensi, J.Y. Koh, Zn²⁺: a novel ionic mediator of neural injury in brain disease, *Trends Pharmacol. Sci.* 21 (2000) 395–401.
- [7] B.K. Bitanirihirwe, M.G. Cunningham, Zinc: the brain's dark horse, *Synapse* 63 (2009) 1029–1049.
- [8] A.S. Nakashima, R.H. Dyck, Zinc and cortical plasticity, *Brain Res. Rev.* 59 (2009) 347–373.
- [9] U. Fegade, H. Sharma, B. Bondhopadhyay, A. Basu, S. Attarde, N. Singh, A. Kuwar, "Turn-on" fluorescent dipodal chemosensor for nano-molar detection of Zn²⁺: application in living cells imaging, *Talanta* 125 (2014) 418–424.
- [10] P. Jiang, Z. Guo, Fluorescent detection of zinc in biological systems: recent development on the design of chemosensors and biosensors, *Coord. Chem. Rev.* 248 (2004) 205–229.
- [11] V. Bhalla, Roopa, M. Kumar, Fluoride triggered fluorescence "turn on" sensor for Zn²⁺ ions based on pentaquinone scaffold that works as a molecular keypad lock, *Org. Lett.* 14 (2012) 2802–2805.
- [12] Y.W. Choi, G.J. Park, Y.J. Na, H.Y. Jo, S.A. Lee, G.R. You, C. Kim, A single schiff base molecule for recognizing multiple metal ions: a fluorescence sensor for Zn(II) and Al(III) and colorimetric sensor for Fe(II) and Fe(III), *Sens. Actuators B* 194 (2014) 343–352.
- [13] E.J. Song, H. Kim, I.H. Hwang, K.B. Kim, A.R. Kim, I. Noh, C. Kim, A single fluorescent chemosensor for multiple target ions: recognition of Zn²⁺ in 100% aqueous solution and F⁻ in organic solvent, *Sens. Actuators B* 195 (2014) 36–43.
- [14] N. Khairnar, K. Tayade, S.K. Sahoo, B. Bondhopadhyay, A. Basu, J. Singh, N. Singh, V. Gite, A. Kuwar, A highly selective fluorescent 'turn-on' chemosensor for Zn²⁺ based on a benzothiazole conjugate: their applicability in live cell imaging and use of the resultant complex as a secondary sensor of CN⁻, *Dalton Trans.* 44 (2015) 2097–2102.
- [15] Y.J. Na, I.H. Hwang, H.Y. Jo, S.A. Lee, G.J. Park, C. Kim, Fluorescent chemosensor based-on the combination of julolidine and furan for selective detection of zinc ion, *Inorg. Chem. Commun.* 35 (2013) 342–345.
- [16] S. Cui, G. Liu, S. Pu, B. Chen, A highly selective fluorescent probe for Zn²⁺ based on a new photochromic diarylethene with a di-2-picolylamine unit, *Dyes Pigm.* 99 (2013) 950–956.
- [17] Y. Li, Q. Zhao, H. Yang, S. Liu, X. Liu, Y. Zhang, T. Hu, J. Chen, Z. Chang, X. Bu, A new ditopic ratiometric receptor for detecting zinc and fluoride ions in living cells, *Analyst* 138 (2013) 5486–5494.
- [18] M. Yan, T. Li, Z. Yang, A novel coumarin Schiff-base as a Zn(II) ion fluorescent sensor, *Inorg. Chem. Commun.* 14 (2011) 463–465.
- [19] H. Kim, J. Kang, K.B. Kim, E.J. Song, C. Kim, A highly selective quinoline-based fluorescent sensor for Zn(II), *Spectrochim. Acta A* 118 (2014) 883–887.
- [20] M. Shamsipur, M. Sadeghi, K. Alizadeh, H. Sharghi, R. Khalifeh, An efficient and selective fluorescent optode membrane based on 7-[(5-chloro-8-hydroxy-7-quinolinyl)methyl]-5,6,7,8,9,10-hexahydro-2H-1,3,4,7,10-benzodioxatriazacyclopentadecine-3,11(4H,12H)-dione as a novel fluorionophore for determination of cobalt(II) ions, *Anal. Chim. Acta* 630 (2008) 57–66.

- [21] G.J. Park, Y.J. Na, H.Y. Jo, S.A. Lee, C. Kim, A colorimetric organic chemo-sensor for Co^{2+} in a fully aqueous environment, *Dalton Trans.* 43 (2014) 6618–6622.
- [22] C. Tsai, Y. Lin, A highly selective and sensitive fluorescence assay for determination of copper(II) and cobalt(II) ions in environmental water and toner samples, *Analyst* 138 (2013) 1232–1238.
- [23] X. Wang, W. Zheng, H. Lin, G. Liu, Y. Chen, J. Fang, A new selective phenanthroline-based fluorescent chemosensor for Co^{2+} , *Tetrahedron Lett.* 50 (2009) 1536–1538.
- [24] F.A. Abebe, C.S. Eribal, G. Ramakrishna, E. Sinn, A 'turn-on' fluorescent sensor for the selective detection of cobalt and nickel ions in aqueous media, *Tetrahedron Lett.* 52 (2011) 5554–5558.
- [25] S.H. Mashraqui, M. Chandiramani, R. Betkar, K. Poonia, A simple internal charge transfer probe offering dual optical detection of Co (II) via color and fluorescence modulations, *Tetrahedron Lett.* 51 (2010) 1306–1308.
- [26] D. Maity, T. Govindaraju, Highly selective colorimetric chemosensor for Co^{2+} , *Inorg. Chem.* 50 (2011) 11282–11284.
- [27] A.R. Khorrami, A.R. Fakhari, M. Shamsipur, H. Naeimi, Pre-concentration of ultra trace amounts of copper, zinc, cobalt and nickel in environmental water samples using modified C18 extraction disks and determination by inductively coupled plasma-optical emission spectrometry, *Environ. Anal. Chem.* 89 (2009) 319–329.
- [28] M. Ghaedi, F. Ahmadi, A. Shokrollahi, Simultaneous preconcentration and determination of copper, nickel, cobalt and lead ions content by flame atomic absorption spectrometry, *J. Hazard. Mater.* 142 (2007) 272–278.
- [29] A. Botcher, T. Takeuchi, K.I. Hardcastle, T.J. Meade, H.B. Gray, Spectroscopy and electrochemistry of cobalt(III) Schiff base complexes, *Inorg. Chem.* 36 (1997) 2498–2504.
- [30] K.S. Rao, T. Balaji, T.P. Rao, Y. Babu, G.R.K. Naidu, Determination of iron, cobalt, nickel, manganese, zinc, copper, cadmium and lead in human hair by inductively coupled plasma-atomic emission spectrometry, *Spectrochim. Acta B* 57 (2002) 1333–1338.
- [31] R.E. Sturgeon, S.S. Berman, A. Desaulniers, D.S. Russell, Determination of iron, manganese, and zinc in seawater by graphite furnace atomic absorption spectrometry, *Anal. Chem.* 51 (1979) 2364–2369.
- [32] R. Gulaboski, V. Mirčeski, F. Scholz, An electrochemical method for determination of the standard Gibbs energy of anion transfer between water and *n*-octanol, *Electrochem. Commun.* 4 (2002) 277–283.
- [33] G.J. Park, Y.J. Na, H.Y. Jo, S.A. Lee, A.R. Kim, I. Noh, C. Kim, A single chemosensor for multiple analytes: fluorogenic detection of Zn^{2+} and OAc^- ions in aqueous solution, and an application to bioimaging, *New J. Chem.* 38 (2014) 2587–2594.
- [34] J. Wang, W. Lin, W. Li, Single fluorescent probe displays a distinct response to Zn^{2+} and Cd^{2+} , *Chem. Eur. J.* 18 (2012) 13629–13632.
- [35] D.T. Quang, J.S. Kim, Fluoro- and chromogenic chemodosimeters for heavy metal ion detection in solution and biospecimens, *Chem. Rev.* 110 (2010) 6280–6301.
- [36] X. Liu, N. Zhang, J. Zhou, T. Chang, C. Fang, D. Shanquan, A turn-on fluorescent sensor for zinc and cadmium ions based on perylene tetracarboxylic diimide, *Analyst* 138 (2013) 901–906.
- [37] Y. Hu, Y. Liu, G. Kim, E.J. Jun, K.M.K. Swamy, Y. Kim, S.-J. Kim, J. Yoon, Pyrene based fluorescent probes for detecting endogenous zinc ions in live cells, *Dyes Pigm.* 113 (2015) 372–377.
- [38] Z. Guo, G.-H. Kim, J. Yoon, I. Shin, Synthesis of a highly Zn^{2+} -selective cyanine-based probe and its use for tracing endogenous zinc ions in cells and organisms, *Nat. Protocol.* 9 (2014) 1245–1254.
- [39] J.Y. Choi, D. Kim, J. Yoon, A highly selective "turn-on" fluorescent chemosensor based on hydroxy pyrene-hydrazone derivative for Zn^{2+} , *Dyes Pigm.* 96 (2013) 176–179.
- [40] Z. Guo, G.-H. Kim, I. Shin, J. Yoon, A cyanine-based fluorescent sensor for detecting endogenous zinc ions in live cells and organisms, *Biomaterials* 33 (2012) 7818–7827.
- [41] (a) Z. Xu, G.-H. Kim, S.J. Han, M.J. Jou, C. Lee, I. Shin, J. Yoon, An NBD-based colorimetric and fluorescent chemosensor for Zn^{2+} and its use for detection of intracellular zinc ions, *Tetrahedron* 65 (2009) 2307–2312; (b) Z. Liu, C. Zhang, Y. Chen, F. Qian, Y. Bai, W. He, Z. Guo, In vivo ratiometric Zn^{2+} imaging in zebrafish larvae using a new visible light excitable fluorescent sensor, *Chem. Commun.* 50 (2014) 1253–1255.
- [42] C. Zhang, Z. Liu, Y. Li, W. He, X. Gao, Z. Guo, *In vitro* and *in vivo* imaging application of a 1,8-naphthalimide-derived Zn^{2+} fluorescent sensor with nuclear envelope penetrability, *Chem. Commun.* 49 (2013) 11430–11432.
- [43] Q. Jiang, Z. Guo, Y. Zhao, F. Wang, L. Mao, *In vivo* fluorescence sensing of the salicylate-induced change of zinc ion concentration in the auditory cortex of rat brain, *Analyst* 140 (2015) 197–203.
- [44] Z. Liu, C. Zhang, Y. Li, Z. Wu, F. Qian, X. Yang, W. He, X. Gao, Z. Guo, A Zn^{2+} fluorescent sensor derived from 2-(pyridin-2-yl)benzimidazole with ratiometric sensing potential, *Org. Lett.* 11 (2009) 795–798.
- [45] F.D. Chaumont, S. Dallongeville, N. Chenouard, N. Hervé, S. Pop, T. Provoost, V. Meas-Yedid, P. Pankajakshan, T. Lecomte, Y.L. Montagner, T. Lagache, A. Dufour, J. Olivia-Marin, Icy: an open bioimage informatics platform for extended reproducible research, *Nat. Methods* 9 (2012) 690–696.
- [46] A.D. Becke, Density-functional thermochemistry. III. The role of exact exchange, *J. Chem. Phys.* 98 (1993) 5648–5652.
- [47] C. Lee, W. Yang, R.G. Parr, Development of the Colle-Salvetti correlation-energy formula into a functional of the electron density, *Phys. Rev. B* 37 (1988) 785–789.
- [48] M.J. Frisch, G.W. Trucks, H.B. Schlegel, G.E. Scuseria, M.A. Robb, J.R. Cheeseman, J.A. Montgomery Jr., T. Vreven, K.N. Kudin, J.C. Burant, J.M. Millam, S.S. Iyengar, J. Tomasi, V. Barone, B. Mennucci, M. Cossi, G. Scalmani, N. Rega, G.A. Petersson, H. Nakatsuji, M. Hada, M. Ehara, K. Toyota, R. Fukuda, J. Hasegawa, M. Ishida, T. Nakajima, Y. Honda, O. Kitao, H. Nakai, M. Klene, X. Li, J.E. Knox, H.P. Hratchian, J.B. Cross, V. Bakken, C. Adamo, J. Jaramillo, R. Gomperts, R.E. Stratmann, O. Yazyev, A.J. Austin, R. Cammi, C. Pomelli, J.W. Ochterski, P.Y. Ayala, K. Morokuma, G.A. Voth, P. Salvador, J.J. Dannenberg, V.G. Zakrzewski, S. Dapprich, A.D. Daniels, M.C. Strain, O. Farkas, D.K. Malick, A.D. Rabuck, K. Raghavachari, J.B. Foresman, J.V. Ortiz, Q. Cui, A.G. Baboul, S. Clifford, J. Cioslowski, B.B. Stefanov, G. Liu, A. Liashenko, P. Piskorz, I. Komaromi, R.L. Martin, D.J. Fox, T. Keith, M.A. Al-Laham, C.Y. Peng, A. Nanayakkara, M. Challacombe, P.M.W. Gill, B. Johnson, W. Chen, M.W. Wong, C. Gonzalez, J.A. Pople, Gaussian 03, Revision D.01, Gaussian Inc., Wallingford, CT, 2004.
- [49] P.C. Hariharan, J.A. Pople, The influence of polarization functions on molecular orbital hydrogenation energies, *Theor. Chim. Acta* 28 (1973) 213–222.
- [50] M.M. Francl, W.J. Pietro, W.J. Hehre, J.S. Binkley, M.S. Gordon, D.F. DeFrees, J.A. Pople, Self-consistent molecular orbital methods. XXIII. A polarization-type basis set for second-row elements, *J. Chem. Phys.* 77 (1982) 3654–3665.
- [51] P.J. Hay, W.R. Wadt, Ab initio effective core potentials for molecular calculations. Potentials for the transition metal atoms Sc to Hg, *J. Chem. Phys.* 82 (1985) 270–283.
- [52] P.J. Hay, W.R. Wadt, Ab initio effective core potentials for molecular calculations. Potentials for main group elements Na to Bi, *J. Chem. Phys.* 82 (1985) 284–298.
- [53] V. Barone, M. Cossi, Quantum calculation of molecular energies and energy gradients in solution by a conductor solvent model, *J. Phys. Chem. A* 102 (1998) 1995–2001.
- [54] M. Cossi, V. Barone, Time-dependent density functional theory for molecules in liquid solutions, *J. Chem. Phys.* 115 (2001) 4708–4717.
- [55] N.M. O'Boyle, A.L. Tenderholt, K.M. Langner, cclib: a library for package-independent computational chemistry algorithms, *J. Comput. Chem.* 29 (2008) 839–845.
- [56] J. Du, J. Fan, X. Peng, H. Li, S. Sun, The quinoline derivative of ratiometric and sensitive fluorescent zinc probe based on deprotonation, *Sens. Actuators B* 144 (2010) 337–341.
- [57] H.G. Lee, J.H. Lee, S.P. Jang, I.H. Hwang, S. Kim, Y. Kim, C. Kim, R.G. Harrison, Zinc selective chemosensors based on the flexible dipicolylamine and quinoline, *Inorg. Chim. Acta* 394 (2013) 542–551.
- [58] Z. Dong, X. Le, P. Zhou, C. Dong, J. Ma, An "off-on-off" fluorescent probe for the sequential detection of Zn^{2+} and hydrogen sulfide in aqueous solution, *New J. Chem.* 38 (2014) 1802–1808.
- [59] S. Aoki, K. Sakurama, N. Matsuo, Y. Yamada, R. Takasawa, S. Tanuma, M. Shiro, K. Takeda, E. Kimura, A new fluorescent probe for zinc(II): an 8-hydroxy-5-*N,N*-dimethylaminosulfonylquinoline-pendant 1,4,7,10-tetraazacyclododecane, *Chem. Eur. J.* 12 (2006) 9066–9080.
- [60] Z. Xu, J. Yoon, D.R. Spring, Fluorescent chemosensors for Zn^{2+} , *Chem. Soc. Rev.* 39 (2010) 1996–2006.
- [61] S. Sinha, G. Dey, S. Kumar, J. Mathew, T. Mukherjee, S. Mukherjee, S. Ghosh, Cysteamine-based cell-permeable Zn^{2+} -specific molecular bioimaging materials: from animal to plant cells, *ACS Appl. Mater. Interfaces* 5 (2013) 11730–11740.
- [62] G.J. Park, H. Kim, J.J. Lee, Y.S. Kim, S.Y. Lee, S. Lee, I. Noh, C. Kim, A highly selective turn-on chemosensor capable of monitoring Zn^{2+} concentrations in living cells and aqueous solution, *Sens. Actuators B* 215 (2015) 568–576.
- [63] N.C. Lim, J.V. Shuster, M.C. Porto, M.A. Tanudra, L. Yao, H.C. Freaque, C. Brückner, Coumarin-based chemosensors for zinc(II): toward the determination of the design algorithm for CHEF-type and ratiometric probes, *Inorg. Chem.* 45 (2005) 2018–2030.
- [64] S. Sinha, T. Mukherjee, J. Mathew, S.K. Mukhopadhyay, S. Ghosh, Triazole-based Zn^{2+} -specific molecular marker for fluorescence bioimaging, *Anal. Chim. Acta* 822 (2014) 60–68.
- [65] P. Job, Formation and stability of inorganic complexes in solution, *Ann. Chim.* 9 (1928) 113–203.
- [66] G. Grynkiewicz, M. Poenie, R.Y. Tseini, A new generation of Ca^{2+} indicators with greatly improved fluorescence properties, *J. Biol. Chem.* 260 (1985) 3440–3450.
- [67] H.Y. Lin, P.Y. Cheng, C.F. Wan, A.T. Wu, A turn-on and reversible fluorescence sensor for zinc ion, *Analyst* 137 (2012) 4415–4417.
- [68] J.H. Kim, I.H. Hwang, S.P. Jang, J. Kang, S. Kim, I. Noh, Y. Kim, C. Kim, R.G. Harrison, Zinc sensors with lower binding affinities for cellular imaging, *Dalton Trans.* 42 (2013) 5500–5507.
- [69] R.M. Harrison, D.P.H. Laxen, S.J. Wilson, Chemical associations of lead, cadmium, copper, and zinc in street dusts and roadside soils, *Environ. Sci. Technol.* 15 (1981) 1378–1383.
- [70] D. Sarkara, A. Pramanik, S. Jana, P. Karmakar, T.K. Mondal, Quinoline based reversible fluorescent 'turn-on' chemosensor for the selective detection of Zn^{2+} : application in living cell imaging and as INHIBIT logic gate, *Sens. Actuators B* 209 (2015) 138–146.
- [71] J.J. Lee, S.A. Lee, H. Kim, L. Nguyen, I. Noh, C. Kim, A highly selective CHEF-type chemosensor for monitoring Zn^{2+} in aqueous solution and living cells, *RSC Adv.* 5 (2015) 41905–41913.
- [72] J.J. Lee, Y.W. Choi, G.R. You, S.Y. Lee, C. Kim, A phthalazine-based two-in-one chromogenic receptor for detecting Co^{2+} and Cu^{2+} in an aqueous environment, *Dalton Trans.* 44 (2015) 13305–13314.

- [73] Y. Leng, F. Zhang, Y. Zhang, X. Fu, Y. Weng, L. Chen, A. Wu, A rapid and sensitive colorimetric assay method for Co^{2+} based on the modified Au nanoparticles (NPs): understanding the involved interactions from experiments and simulations, *Talanta* 94 (2012) 271–277.
- [74] M. Iniya, D. Jeyanthi, K. Krishnaveni, D. Chellappa, Vitamin B6 cofactor based fluorescent probe for sensing an anion (F^-) and cation (Co^{2+}) independently in a pure aqueous medium, *RSC Adv.* 4 (2014) 25393–25397.
- [75] A. Mohamadou, J.-P. Barbiera, J. Marrot, Cobalt(III) complexes with linear hexadentate N_6 or N_4S_2 donor set atoms providing pyridyl–amide–amine/thioether coordination, *Inorg. Chim. Acta* 360 (2007) 2485–2491.
- [76] R. Deblitz, C.G. Hrib, S. Blaurock, P.G. Jones, G. Plenikowski, F.T. Edelmann, Explosive Werner-type cobalt(III) complexes, *Inorg. Chem. Front.* 1 (2014) 621–640.

Biographies

Gyeong Jin Park earned the BS degree in 2013 at Seoul National University of Science and Technology. She is currently a Master Student at Seoul National University of Science and Technology. Her scientific interest includes chemical sensors, synthesis of catalyst and inorganic medicine.

Jae Jun Lee earned the BS degree in 2014 at Seoul National University of Science and Technology. He is currently a Master Student at Seoul National University of Science and Technology. His scientific interest includes, molecular modeling, chemical sensors, and synthesis of catalyst.

Ga Rim You received the BS degree in 2013 at Seoul National University of Science and Technology. He is currently a master student at Seoul National University of Science and Technology. His research interest includes chemical sensors, synthesis of catalyst and metal–organic framework.

LeTuyen Nguyen received the BS degree in 2012 at Ho Chi Minh City University of Technology, a member of Vietnam National University, Ho Chi Minh City. She is currently a Master Student at Seoul National University of Science and Technology. Her research interests focus on tissue engineering.

Insup Noh is currently a Professor at Seoul National University of Science and Technology. He received the PhD degree in 1997 at University of Texas at Austin in USA. He is now interested in development of polymeric biomaterials for local delivery of bioactive agents and tissue engineering of bone, cartilage and nerve.

Cheal Kim is currently a professor at Seoul National University of Science and Technology. He received the PhD degree in 1993 at University of California, San Diego in USA. He is now interested in development of chemical sensors, reactivity study of the transition metal complexes, DNA cleavage by their metal complexes and MOF.